Advances in Nano Research, *Vol. 8 No. 1 (2020) 49-58*
DOI: https://doi.org/10.12989/anr.2020.8.1.049

On transient hygrothermal vibration of embedded viscoelastic flexoelectric/piezoelectric nanobeams under magnetic loading

Ali Shariati [1,2a], Farzad Ebrahimi*[3], Mahsa Karimiasl [3], M. Vinyas [4] and Ali Toghroli**[5]

[1] *Division of Computational Mathematics and Engineering, Institute for Computational Science, Ton Duc Thang University, Ho Chi Minh City, Vietnam*
[2] *Faculty of Civil Engineering, Ton Duc Thang University, Ho Chi Minh City, Vietnam*
[3] *Department of Mechanical Engineering, Faculty of Engineering, Imam Khomeini International University, Qazvin, Iran*
[4] *Department of Aerospace Engineering, Indian Institute of Science, Bangalore-560012, India*
[5] *Institute of Research and Development, Duy Tan University, Da Nang 550000, Vietnam*

(*Received March 24, 2019, Revised September 6, 2019, Accepted December 17, 2019*)

Abstract. This paper investigates the vibration characteristics of flexoelectric nanobeams resting on viscoelastic foundation and subjected to magneto-electro-viscoelastic-hygro-thermal (MEVHT) loading. In this regard, the Nonlocal strain gradient elasticity theory (NSGET) is employed. The proposed formulation accommodates the nonlocal stress and strain gradient parameter along with the flexoelectric coefficient to accurately predict the frequencies. Further, with the aid of Hamilton's principle the governing differential equations are derived which are then solved through Galerkin-based approach. The variation of the natural frequency of MEVHT nanobeams under the influence of various parameters such as the nonlocal strain gradient parameter, different field loads, power-law exponent and slenderness ratio are also investigated.

Keywords: transient damping vibration; magneto-electro-viscoelastic-hygro-thermal; nanobeam; Visco-Pasternak foundation; nonlocal strain gradient elasticity

1. Introduction

Among the numerous smart materials available, an increased application of piezoelectric material can be witnessed due to its extensive beneficial coupling properties. The piezoelectric (PE) material can be incorporated in the smart structures in such a manner that its properties are varied layerwise or gradually along the thickness (Vinyas and Kattimani 2018a, Vinyas *et al*. 2018). More specifically, the researchers have found a significant usage of piezoelectric structures in the engineering applications involving hygrothermal environ-ments. However, the hazardous influence of external moisture and thermal fields can have a deteriorating effect on the structural performance by reducing the stiffness and finally resulting in the failure. Hence, it is very crucial from the designer's view point to predict the structural response of functionally graded (FG) piezoelectric structures very precisely through different computational techniques. In this direction, the influence of loads due to external moisture and thermal fields on FG-PE structures was assessed by Akbarzadeh and Chen (2013). The post-buckling response of FG plates in hygrothermal environment was investigated by Lee and Kim (2013). The effect of thermal and moisture environments on variation of the static parameters of exponentially graded plates was probed by Zenkour (2013). The stability characteristics of auxetic FG plates subjected to hygrothermal loads was studied by Mansouri and Shariyat (2015). Vinyas and Kattimani (2018b) derived a finite element formulation to assess the static behaviour and dynamic analysis (Vinyas and Kattimani 2018c) of FG magneto-electro-elastic plates and beams with different composition of piezoelectric material subjected to various forms of hygrothermal loading. Zghal *et al*. (2018) and Frikha *et al*. (2018) evaluated the stability and dynamic characteristics of FG-CNT composite curved panels, respectively. Meanwhile, Trabelsi *et al*. (2019) evaluated the effect of thermal environment on the stability behaviour of FGM plates and shells. Several papers have been studied the dynamic response of the structures, such as composite structures under seismic events and steel-storage upright sections (Shah *et al*. 2016a, b, Shariati *et al*. 2019a), also different types of loading scenarios as full-cyclic, half cyclic, reversed cyclic, and shack table have employed to evaluate structural behaviour of these specimens in full-scale or half-scale tests (Shariati *et al*. 2012a, 2014, Khorramian *et al*. 2015, Khorami *et al*. 2017).

Several researches have been centered only on the nonlocal elasticity theory (NET) in order to evaluate the mechanical response of nanoplates as a matter of fact that it is convenient to adopt small scale effects. However, the limitation of NET exists in the fact that it does not considers the stiffness increment as observed in experimental works and strain gradient elasticity (Zenkour *et al*. 2014). To overcome this hurdle, many researchers have attempted to

*Corresponding author, Ph.D.,
E-mail: febrahimy@eng.ikiu.ac.ir
**Co-corresponding author, Ph.D. Candidate,
E-mail: alitoghroli@duytan.edu.vn
[a] Ph.D. Candidate, E-mail: alishariati@tdtu.edu.vn

ISSN: 2287-237X (Print), 2287-2388 (Online)

propose different versions of nonlocal strain gradient theory (NSGT). Among them, Lim (2010) and (Ebrahimi and Barati 2016a, b) was successful in incorporating two length scales parameters in NSGT to predict the mechanical response of nanostructures precisely. Further, according to the research on nanobeams by Ebrahimi and Barati (2017a, b), the nonlocal and strain gradient effects significantly influence the stiffness-softening and stiffness-hardening mechanism, respectively. Ebrahimi *et al*. (2016) also incorporated NSGT to nanoplates to probe the wave frequencies. Heidari *et al*. (2015) extended the NSGT and adopted it for the frequency response evaluation of nanoplate made of functionally graded carbon nanotubes (FG-CNT). At the nanoscale, Zhang and Wang (2012) incorporate the surface effect and assessed the vibrations of PE nanofilms through a sandwich-plate model. The influence of elastic foundation on the frequency response of double layered viscoelastic graphene sheets was probed by Hashemi *et al*. (2015). The thermal effect on the frequency of double-viscoelastic FG nanoplates was investigated by Hosseini and Jamalpoor (2015). Among the very limited researches on investigating the hygrothermal effects on nanostructures, Alzahrani *et al*. (2013) studied the static response of nanoplates in hygrothermal environment via NET. Analogously, Sobhy (2015a) studied the dynamic characteristics of graphene sheets subjected to hygrothermal load which was later extended to orthotropic nanoplates (2015b). Also, Active vibration compensator on moving vessel by hydraulic parallel mechanism examined by Tanaka (2018). Through NET, the bending and buckling response of FG nanobeams was studied by Şimşek and Yurtcu (2013) and Mahmoud *et al*. (2015). Rahmani and Pedram (2014) proposed a nonlocal Timoshenko beam model to investigate the vibration response of FG nanobeams. Ebrahimi and Salari (2015a) evaluated the influence of thermal fields on the mechanical response of FG nanobeams considering temperature-dependent properties. Similar investigation was done by Zemri *et al*. (2015) through nonlocal shear deformable refined theory. Ebrahimi and Barati (2015b) also investigated the frequencies of FG nanobeams through the analytical formulation developed on the basis of nonlocal third order beam model. Using NSGT, Li *et al*. (2015) performed wave frequency response analysis for FG nanobeams. Very recently, realizing the benefits of viscoelastic materials and elastic mediums in vibration damping Lei *et al*. (2013) analyzed vibrations of size-dependent Kelvin–Voigt viscoelastic damped nanobeams. However, to the best knowledge of the authors, no study has focused on hygro-thermal vibrational response of two-variable sinusoidal shear deformation viscoelastic nanoplates resting on three-parameter viscoelastic foundation based on nonlocal strain gradient theory. Numerous techniques have been conducted for data validations and predictions such as employing artificial neural networks (Safa *et al*. 2016, 2020, Sedghi *et al*. 2018, Xu *et al*. 2019, Trung *et al*. 2019, Shariati *et al*. 2020), Finite element method (Shariati *et al*. 2012b, 2019b, Shahabi *et al*. 2016), Finite strip method (Daie *et al*. 2011, Jalali *et al*. 2012, Zandi *et al*. 2018). Finite element method which is generally carried out by FE programs as ABAQUS and ANSYS performed as a reliable technique for empirical data validation and response prediction.

In this paper the transient damping vibration of magneto-electro-viscoelastic-hygro-thermal (MEVHT) nanobeams accommodated in viscoelastic foundation based on nonlocal strain gradient elasticity. To this end, Higher-order refined beam theories used for the displacement components. The viscoelastic foundation is made of Winkler-Pasternak layer. Power-law model is adopted to describe the continuous variation of temperature-dependent material properties of nanobeam. The governing equations of nonlocal strain gradient viscoelastic nanobeam are obtained by Hamilton's principle and solved through an analytical solution for different boundary conditions. A parametric study is presented to inquire the effect of the nonlocal strain gradient parameter, hygro-thermo-magneto-electro-mechanical loadings on the vibration characteristics of MEVHT nanobeams. The influence of the mechanical loading, electric loading and magnetic loading; power-law exponent and slenderness ratio on the frequency response of viscoelastic nanobeams are studied thoroughly. Moreover, the tricky empirical experiments have always been a barrier in front of the new explorations; however, employing intelligence solutions are one of the practical ways to address these issues. Whereas, artificial intelligence techniques have perfomed on a variety of experimental studies and proved to be reliable not only in case of parameters estimation but also the prediction of crucial design characteristics (Shao *et al*. 2018, Li *et al*. 2019, Luo *et al*. 2019, Milovancevic *et al*. 2019, Shi *et al*. 2019a, b, Suhatril *et al*. 2019). Different kind of algorithms has introduced which have their traits and advantages (Mansouri *et al*. 2019, Xu *et al*. 2019). Using the relevant algorithms in order to analytical assessment has been carried out on different types of studies (Safa *et al*. 2016, Sedghi *et al*. 2018). That being the case, performing the artificial intelligence algorithms is a potential method to avoid non-linearity and sophisticated analysis of the nanoscale problems.

2. Theory and formulation

2.1 Kinematic relations

The kinematics displacements of MEVHT nanobeam can be expressed through refined shear deformable model by

$$\boldsymbol{u_x(x,z_{ns})=u(x)-z_{ns}\frac{\partial w_b}{\partial x}-f(z_{ns})\frac{\partial w_s}{\partial x}} \quad (1)$$

$$\boldsymbol{u_z(x,z_{ns})=w_b(x)+w_s(x)} \quad (2)$$

in which, u, w_b, w_s are the axial mid-plane displacement, bending and shear components of transverse displacement, respectively.

$$f(z_{ns})=z_{ns}+h_0-tan[\,m(z_{ns}+h_0)], m=0.03 \quad (3)$$

where, $f(z_{ns})$ is the shape function. In the present study, $f(z_{ns})$ signifies the distribution of shear stress/strain across

the beam thickness. Since, a trigonometric variation is assumed in the current work, the necessity of shear correction factor can be eliminated (Sobhy 2015b).

For the proposed beam model, the non-zero strains are represented as follows

$$\varepsilon_{xx} = \frac{\partial u}{\partial x} - z_{ns}\frac{\partial^2 w_b}{\partial x^2} - f(z_{ns})\frac{\partial^2 w_s}{\partial x^2} \tag{4}$$

$$\gamma_{xz} = g(z_{ns})\frac{\partial w_s}{\partial x} \tag{5}$$

Where $g(z_{ns}) = 1 - \frac{df(z_{ns})}{dz_{ns}}$. Also, the Hamilton's principle states that

$$\int_0^t \delta(\Pi_S - \Pi_K + \Pi_W)\mathrm{d}t = 0 \tag{6}$$

where Π_S is the total strain energy, Π_K is the kinetic energy and Π_W is the work done by external applied forces. The first variation of strain energy Π_S can be calculated as

$$\delta\Pi_S = \int \sigma_{ij}\delta\varepsilon_{ij}dv = \int \sigma_x\delta\varepsilon_x + \sigma_{xz}\delta\gamma_{xz} + \sigma_{yz}\delta\gamma_{yz} \tag{7}$$

Substituting Eqs. (1)-(2) into Eq.(6) yields

$$\begin{aligned}\delta\Pi_S = \int_0^l (&N\frac{\partial\delta u}{\partial x} - M_b\frac{\partial^2\delta w_b}{\partial x^2} - M_s\frac{\partial^2\delta w_s}{\partial x^2}\\ &+Q\frac{\partial\delta w_s}{\partial x})dx\end{aligned} \tag{8}$$

In which the forces and moments expressed in the above equation are defined as follows

$$\begin{aligned}(N, M_b, M_s) &= \int_{-\frac{h}{2}-h_0}^{\frac{h}{2}-h_0}(1, z_{ns}, f)\sigma_{xx}\,dz_{ns}, Q\\ &= \int_{-h/2-h_0}^{h/2-h_0} g\sigma_{xz}\,dA\end{aligned} \tag{9}$$

In this study, the nanobeam is subjected to an in-plane axial magnetic field. Hence, to derive the exerted body force from longitudinal magnetic field$H = (H_x, 0,0)$, the Maxwell relations are adopted

$$f_{Lz} = \eta(\nabla \times (\nabla \times (\vec{u} \times \vec{H}))) \times \vec{H} \tag{10}$$

where $\vec{u} = (u_x, 0, u_z)$ is displacement vector and η is magnetic parliamentary. For a planar beam deformation with the assumed displacement field, the resultant Lorentz force takes the form

$$f_{Lz} = \eta\int_A f_z\,dA = \eta AH_x^2\frac{\partial^2 w}{\partial x^2} \tag{11}$$

The first variation of the work done by applied forces can be written in the form

$$\begin{aligned}\delta\Pi_w = \int_0^l [&-N_x^0\frac{\partial w^b}{\partial x}\frac{\partial\delta w^b}{\delta x}\\ &-N_y^0\frac{\partial w^s}{\partial y}\frac{\partial\delta w^s}{\delta y} + 2\delta N_{xy}^0\frac{\partial w^b}{\partial x}\frac{\partial w^s}{\delta y}\\ &-k_w\delta(w^b + w^s) + k_p\partial^2\frac{(w_{b+}w_{s)}}{\partial x^2}]dx\\ &-c_d\frac{\partial\delta(w^b + w^s)}{\delta t}\\ &-\eta AH_x^2\frac{\partial^2\delta(w^b + w^s)}{\partial x^2} + f_{13}\delta(w^b + w^s)\end{aligned} \tag{12}$$

Where N^T, N^H, f_{13} are flexoelectricity coefficient, applied forces due to variation of temperature and moisture as

$$\begin{aligned}N^T &= \int_{-h/2-h_0}^{h/2-h_0} E(z_{ns})\alpha(z_{ns})(\Delta T)dz_{ns},\\ N^H &= \int_{-h/2-h_0}^{h/2-h_0} E(z_{ns})\beta(z_{ns})(\Delta H)dz_{ns}\end{aligned} \tag{13}$$

Where $\Delta T = T - T_0$ and $\Delta H = H - H_0$ in which T_0 and H_0 are the reference temperature and moisture concentration, respectively, where k_w, k_p and c_d are linear, shear and damping coefficients of medium, respectively. The variation of kinetic energy is represented by

$$\begin{aligned}\delta\Pi_k = \int_0^l I_0\Big[&\frac{\partial u}{\partial t}\frac{\partial\delta u}{\partial t} + \left(\frac{\partial w_b}{\partial t} + \frac{\partial\delta w_s}{\delta t}\right)\left(\frac{\partial w_b}{\partial t} + \frac{\partial\delta w_s}{\delta t}\right)\\ &-I_1\left(\frac{\partial u}{\partial t}\frac{\partial^2\delta w_b}{\partial x\partial t} + \frac{\partial\delta u}{\partial t}\frac{\partial^2 w_b}{\delta x\partial t}\right)\\ &+I_2\left(\frac{\partial^2 w_b}{\partial x\partial t}\frac{\partial^2\delta w_b}{\partial x\partial t}\right)\Big]\\ &-J_1\left(\frac{\partial u}{\partial t}\frac{\partial^2\delta w^s}{\partial x\partial t} + \frac{\partial\delta u}{\partial t}\frac{\partial^2 w_s}{\delta x\partial t}\right)\\ &+K_2\left(\frac{\partial^2 w_s}{\partial x\partial t}\frac{\partial^2\delta w_s}{\partial x\partial t}\right)\\ &+J_2\left(\frac{\partial^2 w_b}{\partial x\partial t}\frac{\partial^2\delta w_s}{\partial x\partial t} + \frac{\partial^2 w_s}{\partial x\partial t}\frac{\partial^2\delta w_b}{\partial x\partial t}\right)\end{aligned} \tag{14}$$

where

$$\begin{aligned}&(I_0, I_1, J_1, I_2, J_2, K_2)\\ &= \int_{-h/2-h_0}^{h/2-h_0}\rho(z_{ns})(1, z_{ns}, f, z_{ns}^2, z_{ns}f, f^2)dz_{ns}\end{aligned} \tag{15}$$

The governing equations are obtained by inserting Eqs. (9)-(16) in Eq. (8) when the coefficients of $\delta u, \delta w_b$ and δw_s are equal to zero

$$\frac{\partial N}{\partial x} = I_0\frac{\partial^2 u}{\partial t^2} - I_1\frac{\partial^3 w_b}{\partial x\partial t^2} - J_1\frac{\partial^3 w_s}{\partial x\partial t^2} - \eta AH_x^2(w^b + w^s) \tag{16}$$

$$\begin{aligned}\frac{\partial^2 M_b}{\partial x^2} = &(N^T + N^H)\frac{\partial^2(w_b + w_s)}{\partial x^2} + I_0\left(\frac{\partial^2 w_b}{\partial t^2} + \frac{\partial^2 w_s}{\partial t^2}\right)\\ &+I_1\frac{\partial^3 u}{\partial x\partial t^2} - I_2\frac{\partial^4 w_b}{\partial x^2\partial t^2} - J_2\frac{\partial^4 w_s}{\partial x^2\partial t^2}\\ &+k_w(w_b + w_s) - k_p\frac{\partial^2(w_b + w_s)}{\partial x^2} + c_d\frac{\partial(w_b + w_s)}{\partial t}\end{aligned} \tag{17}$$

$$\begin{aligned}\frac{\partial^2 M_s}{\partial x^2}+\frac{\partial Q}{\partial x} &= (N^T+N^H)\frac{\partial^2(w_b+w_s)}{\partial x^2}\\ &+I_0\left(\frac{\partial^2 w_b}{\partial t^2}+\frac{\partial^2 w_s}{\partial t^2}\right)+J_1\frac{\partial^3 u}{\partial x\partial t^2}\\ &-J_2\frac{\partial^4 w_b}{\partial x^2\partial t^2}-K_2\frac{\partial^4 w_s}{\partial x^2\partial t^2}\\ &+k_w(w_b+w_s)-k_p\frac{\partial^2(w_b+w_s)}{\partial x^2}\\ &+c_d\frac{\partial(w_b+w_s)}{\partial t}\end{aligned} \tag{18}$$

2.2 The nonlocal strain gradient elasticity model for FGM nanobeams

Based on nonlocal strain gradient theory, the stress accounts for both nonlocal elastic stress field and the strain gradient stress field. Hence, the stress can be expressed by

$$\sigma_{ij}=\sigma_{ij}^{(0)}-\frac{d\sigma_{ij}^{(1)}}{dx} \tag{19}$$

Where the stress $\sigma_{xx}^{(0)}$ corresponds to strain ε_{xx} and higher order stress $\sigma_{xx}^{(1)}$ corresponds to strain gradient $\varepsilon_{xx,x}$ and are defined by

$$\sigma_{ij}^{(0)}=\int_0^L C_{ijkl}\,\alpha_0(x,x',e_0a)\varepsilon_{kl}'(x')dx' \tag{20}$$

$$\sigma_{ij}^{(1)}=l^2\int_0^L C_{ijkl}\,\alpha_1(x,x',e_1a)\varepsilon_{kl,x}'(x')dx' \tag{21}$$

In which $C_{ijkl}$are the elastic constants and e_0a and e_1a consider the influences of nonlocal stress field, and $l$denote the material length scale parameter and captures the effects of higher-order strain gradient stress field.

$$\begin{aligned}&[1-(e_1a)^2\nabla^2][1-(e_0a)^2\nabla^2]\sigma_{ij}\\ &=C_{ijkl}[1-(e_1a)^2\nabla^2]\varepsilon_{kl}\\ &-C_{ijkl}l^2[1-(e_0a)^2\nabla^2]\nabla^2\varepsilon_{kl}\end{aligned} \tag{22}$$

The constitutive Eq. (23) can be developed to capture the influence of hygro-thermal loading as

$$\begin{aligned}&\sigma_{ij}-(ea)^2\nabla^2\sigma_{ij}\\ &=1-l^2\nabla^2\begin{bmatrix}C_{ijkl}\varepsilon_{kl}-f_{klij}\dfrac{\partial_{E_K}}{\partial x_l}+C_{ijkl}\alpha_{kl}\\ -C_{ijkl}\beta_{kl}\Delta H-\eta AH_x^2\end{bmatrix}\end{aligned} \tag{23}$$

where α_{ij} and β_{ij} are thermal and moisture expansion coefficients, respectively; T and H denote the temperature and moisture variation, respectively. Thus, the constitutive relations for a nonlocal refined shear deformable FG nanobeam can be stated as

$$\begin{aligned}&\sigma_{xx}-\mu\frac{\partial^2\sigma_{xx}}{\partial x^2}\\ &=E(Z_{ns})\left(\varepsilon_{xx}-\eta\frac{\partial^2\varepsilon_{xx}}{\partial x^2}-\alpha\Delta T-\beta\Delta H-f_{lz}\right)\end{aligned} \tag{24a}$$

$$\sigma_{xz}-\mu\frac{\partial^2\sigma_{xz}}{\partial x^2}=G(z_{ns})(\gamma_{xz}-\eta\frac{\partial^2\gamma_{xz}}{\partial x^2}) \tag{24b}$$

Where $\mu=ea^2$ and $\eta=l^2$. Applying the Kelvin's model on elastic materials with viscoelastic structural damping coefficient (g) and integrating Eq. (24) over the cross-section area of nanobeam provides the following nonlocal relations for a refined FGM beam model as

$$\begin{aligned}&N-\mu\frac{\partial^2 N}{\partial x^2}=\left(1-\eta\frac{\partial^2}{\partial x^2}\right)\left(1+g\frac{\partial}{\partial t}\right)\\ &\left(A\frac{\partial u}{\partial x}-B\frac{\partial^2 w_b}{\partial x^2}-B_S\frac{\partial^2 w_s}{\partial x^2}\right)-N_x^T-N_x^H\end{aligned} \tag{25}$$

$$\begin{aligned}&M_b-\mu\frac{\partial^2 M_b}{\partial x^2}=\left(1-\eta\frac{\partial^2}{\partial x^2}\right)\left(1+g\frac{\partial}{\partial t}\right)\\ &\left(B\frac{\partial u}{\partial x}-D\frac{\partial^2 w_b}{\partial x^2}-D_s\frac{\partial^2 w_s}{\partial x^2}\right)-M_b^T-M_b^H\end{aligned} \tag{26}$$

$$\begin{aligned}&M_s-\mu\frac{\partial^2 M_s}{\partial x^2}=\left(1-\eta\frac{\partial^2}{\partial x^2}\right)\left(1+g\frac{\partial}{\partial t}\right)\\ &\left(B_s\frac{\partial u}{\partial x}-D_s\frac{\partial^2 w_b}{\partial x^2}-H_s\frac{\partial^2 w_s}{\partial x^2}\right)-M_s^T-M_s^H\end{aligned} \tag{27}$$

$$Q-\mu\frac{\partial^2 Q}{\partial x^2}=\left(1-\eta\frac{\partial^2}{\partial x^2}\right)\left(1+g\frac{\partial}{\partial t}\right)\left(A_s\frac{\partial w_s}{\partial x}\right) \tag{28}$$

Where the cross-sectional rigidities are calculated as follows

$$\begin{aligned}&(A,B,B_s,D,D_s,H_s)\\ &=\int_{-h/2-h_0}^{h/2-h_0}E(z_{ns})(1,z_{ns},f,{z_{ns}}^2,z_{ns}f,f^2)\,dz_{ns}\end{aligned} \tag{29}$$

$$A_s=\int_{-h/2-h_0}^{h/2-h_0}g^2G(z_{ns})\,dz_{ns} \tag{30}$$

And

$$\begin{aligned}\{N_x^T,M_b^T,M_s^T\}&=\int_{-\frac{h}{2}-h_0}^{\frac{h}{2}-h_0}E(z_{ns})\alpha(z_{ns})\\ &(T-T_0)\{1,z_{ns},f\}dz_{ns},\\ \{N_x^H,M_b^H,M_s^H\}&=\int_{-\frac{h}{2}-h_0}^{\frac{h}{2}-h_0}E(z_{ns})\beta(z_{ns})\\ &(H-H_0)\{1,z_{ns},f\}dz_{ns}\end{aligned} \tag{31}$$

The governing equations of shear deformable viscoelastic nanobeam resting on three-parameter viscoelastic medium in hygro-thermal environment in terms of displacements are obtained by inserting for N, M_b, M_s and Q from Eqs. (25)-(28), respectively into Eqs. (16)-(18) as follows

$$\begin{aligned}&A\left(1-\eta\frac{\partial^2}{\partial x^2}\right)\left(\frac{\partial^2 u}{\partial x^2}+g\frac{\partial^3 u}{\partial t\partial x^2}\right)\\ &-B\left(1-\eta\frac{\partial^2}{\partial x^2}\right)\left(\frac{\partial^3 w_b}{\partial x^3}+g\frac{\partial^4 w_b}{\partial t\partial x^3}\right)\\ &-B_s\left(1-\eta\frac{\partial^2}{\partial x^2}\right)\left(\frac{\partial^3 w_s}{\partial x^3}+g\frac{\partial^4 w_s}{\partial t\partial x^3}\right)\end{aligned} \tag{32}$$

$$-I_0\frac{\partial^2 u}{\partial t^2}+I_1\frac{\partial^3 w_b}{\partial x\partial t^2}+J_1\frac{\partial^3 w_s}{\partial x\partial t^2}+\mu\left(I_0\frac{\partial^4 u}{\partial x^2\partial t^2}-I_1\frac{\partial^5 w_b}{\partial x^3\partial t^2}-J_1\frac{\partial^5 w_s}{\partial x^3\partial t^2}\right)=0 \tag{32}$$

$$\begin{aligned}&B\left(1-\eta\frac{\partial^2}{\partial x^2}\right)\left(\frac{\partial^3 u}{\partial x^3}+g\frac{\partial^4 u}{\partial t\partial x^3}\right)\\&-D\left(1-\eta\frac{\partial^2}{\partial x^2}\right)\left(\frac{\partial^4 w_b}{\partial x^4}+g\frac{\partial^5 w_b}{\partial t\partial x^4}\right)\\&-D_s\left(1-\eta\frac{\partial^2}{\partial x^2}\right)\left(\frac{\partial^4 w_s}{\partial x^4}+g\frac{\partial^5 w_s}{\partial t\partial x^4}\right)\\&-(N^T+N^H)\frac{\partial^2(w_b+w_s)}{\partial x^2}-I_0\left(\frac{\partial^2 w_b}{\partial t^2}+\frac{\partial^2 w_s}{\partial t^2}\right)\\&-I_1\frac{\partial^3 u}{\partial x\partial t^2}+I_2\frac{\partial^4 w_b}{\partial x^2\partial t^2}+J_2\frac{\partial^4 w_s}{\partial x^2\partial t^2}\\&-k_w(w_b+w_s)+k_p\frac{\partial^2(w_b+w_s)}{\partial x^2}\\&-c_d\frac{\partial(w_b+w_s)}{\partial t}+\mu\left((N^T+N^H)\frac{\partial^4(w_b+w_s)}{\partial x^4}\right.\\&+I_0\left(\frac{\partial^4 w_b}{\partial x^2\partial t^2}+\frac{\partial^4 w_s}{\partial x^2\partial t^2}\right)\\&+I_1\frac{\partial^5 u}{\partial x^3\partial t^2}-I_2\frac{\partial^6 w_b}{\partial x^4\partial t^2}-J_2\frac{\partial^6 w_s}{\partial x^4\partial t^2}\\&+k_w\frac{\partial^2(w_b+w_s)}{\partial x^2}-k_p\frac{\partial^4(w_b+w_s)}{\partial x^4}\\&\left.+c_d\frac{\partial^3(w_b+w_s)}{\partial x^2\partial t}\right)=0\end{aligned} \tag{33}$$

$$\begin{aligned}&B_s\left(1-\eta\frac{\partial^2}{\partial x^2}\right)\left(\frac{\partial^3 u}{\partial x^3}+g\frac{\partial^4 u}{\partial t\partial x^3}\right)\\&-D_s\left(1-\eta\frac{\partial^2}{\partial x^2}\right)\left(\frac{\partial^4 w_b}{\partial x^4}+g\frac{\partial^5 w_b}{\partial t\partial x^4}\right)\\&-H_s\left(1-\eta\frac{\partial^2}{\partial x^2}\right)\left(\frac{\partial^4 w_s}{\partial x^4}+g\frac{\partial^5 w_s}{\partial t\partial x^4}\right)\\&+A_S\left(1-\eta\frac{\partial^2}{\partial x^2}\right)\left(\frac{\partial^2 w_s}{\partial x^2}+g\frac{\partial^3 w_s}{\partial t\partial x^2}\right)\\&-I_0\left(\frac{\partial^2 w_b}{\partial t^2}+\frac{\partial^2 w_s}{\partial t^2}\right)-J_1\frac{\partial^3 u}{\partial x\partial t^2}+J_2\frac{\partial^4 w_b}{\partial x^2\partial t^2}\\&+k_2\frac{\partial^4 w_s}{\partial x^2\partial t^2}-k_w(w_b+w_s)-\eta AH_x^2(w^b+w^s)\\&+k_p\frac{\partial^2(w_b+w_s)}{\partial x^2}-c_d\frac{\partial(w_b+w_s)}{\partial t}\\&+\mu((N^T+N^H)\frac{\partial^4(w_b+w_s)}{\partial x^4}+I_0\left(\frac{\partial^4 w_b}{\partial x^2\partial t^2}+\frac{\partial^4 w_s}{\partial x^2\partial t^2}\right)\\&+J_1\frac{\partial^3 u}{\partial x^3\partial t^2}-J_2\frac{\partial^6 w_b}{\partial x^4\partial t^2}+k_2\frac{\partial^6 w_s}{\partial 4\partial t^2}+k_w\frac{\partial^2(w_b+w_s)}{\partial x^2}\\&+k_p\frac{\partial^4(w_b+w_s)}{\partial x^4}+\eta AH_x^2\frac{\partial^2(w_b+w_s)}{\partial x^2}\\&+c_d\frac{\partial^3(w_b+w_s)}{\partial x^2\partial t}-\frac{e_{31}}{2k_{33}}f_{13}\left(\frac{\partial^2 w_b}{\partial x^2}+\frac{\partial^2 w_s}{\partial x^2}\right)\end{aligned} \tag{34}$$

3. Solution procedure

In this section, an analytical solution is implemented in which the generalized displacements are expanded in a double Fourier series in terms of unknown parameters. The selection of the functions in these series is associated to those which satisfy the boundary edges of the nanoplate. These boundary edges are given as :

- Simply-supported (S):

$$w_b=w_s=N_x=M_x=0 \qquad \text{at} \qquad x=0,a \tag{35}$$

$$w_b=w_s=N_y=M_y=0 \qquad \text{at} \qquad y=0,b \tag{36}$$

- Clamped (C):

$$\begin{aligned}&u=v=w_b=w_s=0\\&\text{at}\quad x=0,a\quad\text{and}\quad y=0,b\end{aligned} \tag{37}$$

To satisfy above-mentioned boundary conditions, the displacement quantities are presented in the following form

$$u=\sum_{m=1}^{\infty}\sum_{n=1}^{\infty}U_{mn}\frac{\partial X_m(x)}{\partial x}Y_n(y) \tag{38}$$

$$w_b=\sum_{m=1}^{\infty}\sum_{n=1}^{\infty}W_{bmn}X_m(x)\,Y_n(y) \tag{39}$$

$$w_s=\sum_{m=1}^{\infty}\sum_{n=1}^{\infty}W_{smn}X_m(x)\,Y_n(y) \tag{40}$$

where (U_{mn}, W_{bmn}, W_{zmn}) are the unknown coefficients and for different boundary conditions ($\alpha=m\pi/a$, $\beta=n\pi/b$).
where

$$\{[K]+[C]\omega+[M]\omega^2\}\begin{Bmatrix}U_n\\W_{bn}\\W_{sn}\end{Bmatrix}=0 \tag{41}$$

Where [K], [C] and [M] are the stiffness, damping, and mass matrixes for FG nanobeam, respectively.

$$\begin{aligned}k_{1,1}&=A(\alpha_3-\eta\alpha_{11}),\\K_{1,2}&=B(\alpha_9-\eta\alpha_{13}),\\K_{1,3}&=B_S(\alpha_9-\eta\alpha_{13})\\k_{2,3}&=\left(N^H+N^T-k_p\right)(-\alpha_7+\mu\alpha_9)-k_w(\alpha_5-\mu\alpha_7)\\&\quad-f_{lz}(\alpha_5-\mu\alpha_7)-D_s(\alpha_9-\eta\alpha_{13})\\K_{2,2}&=\left(N^H+N^T-k_p\right)(-\alpha_7+\mu\alpha_9)-k_w(\alpha_5-\mu\alpha_7)\\&\quad-f_{lz}(\alpha_5-\mu\alpha_7)-D(\alpha_9-\eta\alpha_{13})\\K_{3,3}&=\left(N^H+N^T-k_p\right)(-\alpha_7+\mu\alpha_9)-k_w(\alpha_5-\mu\alpha_7)\\&\quad-A_s(\alpha_5-\mu\alpha_7)-\frac{e_{31}}{2k_{33}}f_{13}(\alpha_5-\mu\alpha_7)\\&\quad-H_s(\alpha_9-\eta\alpha_{13})\\c_{1,1}&=Aig(\alpha_3-\eta\alpha_{11}),\\c_{1,2}&=Big(\alpha_9-\eta\alpha_{13}),\\c_{1,3}&=B_s\,ig(\alpha_9-\eta\alpha_{13})\\c_{3,3}&=-c_di(\alpha_5-\mu\alpha_7)+A_sig(\alpha_7-\mu\alpha_9)\\&\quad-H_s(\alpha_9-\eta\alpha_{13})\end{aligned} \tag{42}$$

Table 1 Flexoelectric properties of PZT-5H sandwich beam

Properties	PZT-5H
c_{11} (Gpa)	102
c_{12}	31
c_{66}	35.5
e_{31} (C/m^2)	17.05
k_{33} (C/(Vm))	1.76 × 10^{-8}
f_{31} (V)	10^{-7}
c_{11}^s (N/m)	102
c_{12}^s	3.3
c_{66}^s	2.13
e_{31}^s (C/m)	-3.8 × 10^{-8}

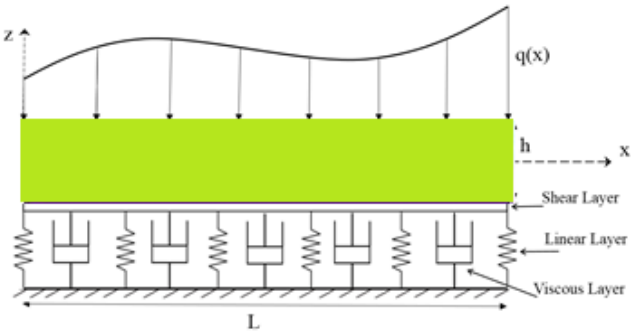

Fig. 1 Geometry of MEVHT nanobeam resting on viscoelastic foundation

$$\begin{aligned} m_{1,1} &= (\alpha_1 - \eta\alpha_3)I_0, \\ m_{1,2} &= (\alpha_7 - \eta\alpha_9)I_1, \\ m_{1,3} &= (\alpha_7 - \eta\alpha_9)J_1 \\ m_{2,2} &= (\alpha_5 - \eta\alpha_7)I_0 - (\alpha_7 - \eta\alpha_9)I_2, \\ m_{2,3} &= (\alpha_5 - \eta\alpha_7)I_0 - (\alpha_7 - \eta\alpha_9)J_2 \\ m_{3,3} &= (\alpha_5 - \eta\alpha_7)I_0 - (\alpha_7 - \eta\alpha_9)k_2 \end{aligned} \tag{42}$$

In which

$$\alpha_1 = \int_0^L X_m' X_m' dx, \alpha_3 = \int_0^L X_m''' X_m' \, dx \tag{43}$$

$$\begin{aligned} \alpha_5 &= \int_0^L X_m X_m dx, \alpha_7 = \int_0^L X_m'' X_m \, dx, \alpha_9 \\ &= \int_0^L X_m'''' X_m \, dx \end{aligned} \tag{44}$$

$$\alpha_{11} = \int_0^L X_m'''' X_m' dx, \alpha_{13} = \int_0^L X_m''''' X_m \, dx \tag{45}$$

4. Numerical results and discussions

In this section the damped frequency response of MEVHT nanobeams are depicted through several set of illustrations considering various boundary conditions (S-S and C-C). The material properties adopted for MEVHT nanobeam are shown in Table 1. Unless and otherwise mentioned, the specifications of MEVHT nanobeams considered in this analysis are as follows: L = 10 nm, L/h = 20, ΔT = 20, ΔH = 1, $K_w = K_p$ = 0.

The frequencies are evaluated in the dimensionless form with the aid of dimensionless viscoelastic parameters that can be represented as follows

$$\begin{aligned} &\widetilde{\omega} = \omega L^2 \sqrt{\frac{\rho_c A}{E_c I}}, \quad K_w = k_w \frac{L^4}{E_c I}, \quad K_p = k_p \frac{L^2}{E_c I}, \\ &C = c_d \frac{L^2}{\sqrt{E_c I \rho_c A}}, \quad G = \frac{g}{L^2} \sqrt{\frac{E_c I}{\rho_c A}} \end{aligned} \tag{46}$$

Figs. 2 and 3 show the effects of nonlocal parameter (μ) and length scale parameter (η) on damping frequency of MEVHT nanobeams, respectively. It is observable from Fig. 2 that with the higher nonlocal parameter (μ), the imaginary part (IP) and real part (RP) of eigen frequency reduces. Further, the critical damping co-efficient reduces for higher values of μ.

From Fig. 3, it can be witnessed that with a higher value of length scale parameter (η) the critical point move towards right. The value of critical damping coefficient reduces indicating that the critical damping coefficient for the nonlocal elasticity beam model is lesser that that of nonlocal strain gradient beam model. Meanwhile, the μ

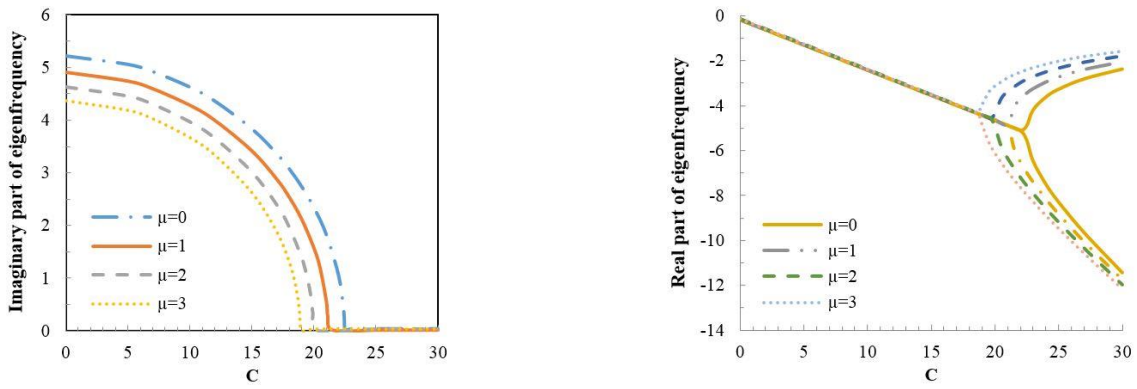

Fig. 2 Effect of μ on (a) IP of eigen frequency; (b) RP of eigen frequency of MEVHT nanobeam (L/h = 10, p = 1, ΔT = 20, ΔH = 1, η = 0, $K_w = K_p$ = 0)

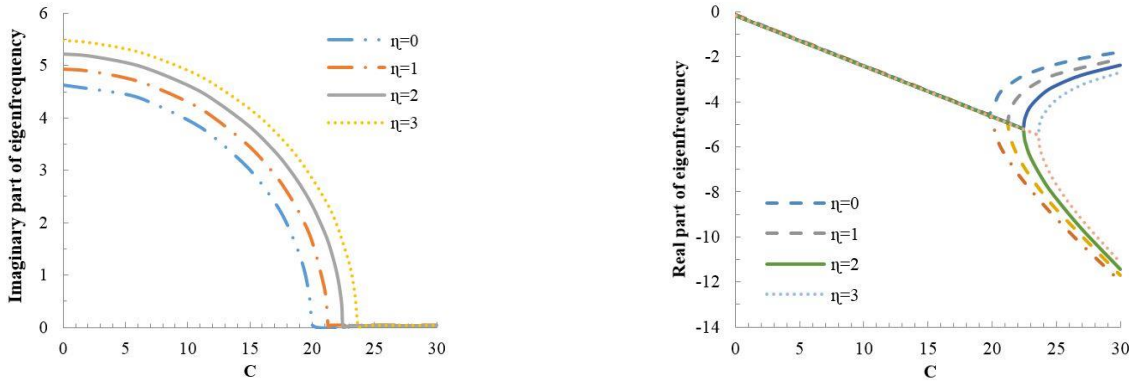

Fig. 3 Effect of η on (a) IP of eigen frequency; (b) RP of eigen frequency of MEVHT nanobeam (L/h = 10, p = 1, ΔT = 20, ΔH = 1, η = 0, K_w = K_p = 0)

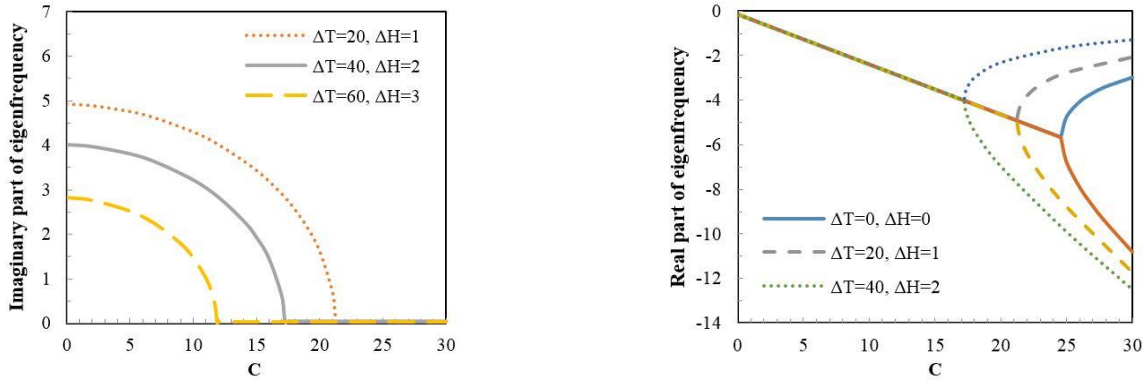

Fig. 4 Effect of hygrothermal loads on (a) IP of eigen frequency; (b) RP of eigen frequency of MEVHT nanobeam (L/h = 10, ΔT = 20, ΔH = 1, K_w = 50, K_p = 10, μ = 2, h = 1)

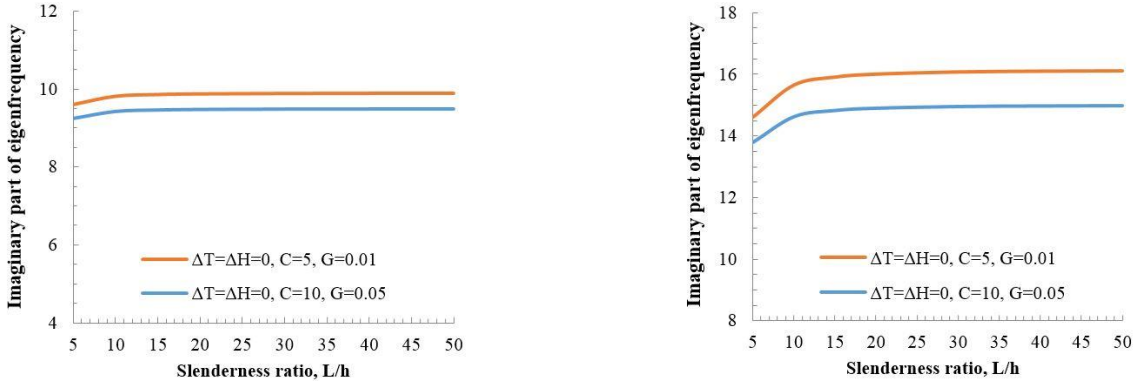

(a) S-S (b) C-C

Fig. 5 Influence of slenderness ratio on the vibration behavior of the FGM viscoelastic nanobeams for various damping coefficients without and with hygro-thermal loading: (a) S-S; (b) C-C boundary condition (K_w = 50, K_p = 10, p = 1, μ = 2, h = 1)

and η has a negligible influence on the real part of frequency at smaller damping coefficient. However, its effect on real eigen frequency becomes significant at larger damping coefficients.

The effect of different magnitudes of hygrothermal loads on the vibration behavior of MEVHT nanobeams at an internal damping (G) of 0.01 is presented in Fig. 4. It can be witnessed from this figure that larger magnitude of moisture (ΔH) and temperature gradient (ΔT) yields a smaller critical damping coefficient.

Fig. 5 shows the influence of slenderness ratio (L/h) on the imaginary frequencies of MEVHT nanobeams. The effect of hygro-thermal loads are nullified in this study. Also, S-S and C-C boundary conditions are considered. It can be observed from these figures that for both the boundary condition considered, the variation of the

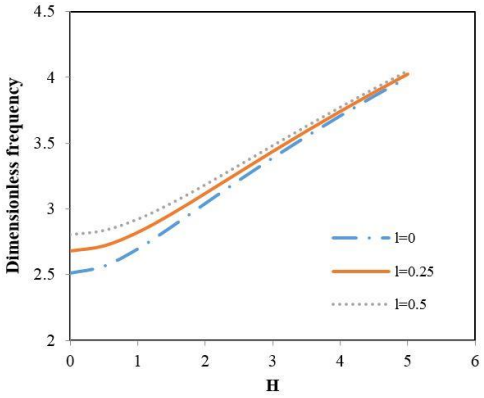

Fig. 6 Effect of magnetic field intensity on the dimensionless frequency of MEVHT nanobeam for different length scale parameters (L/h = 30, Kp = Kw = 0)

imaginary frequencies are negligible at lower slenderness ratios, while it becomes prominent at larger values of slenderness ratio. Also, a higher damping coefficient yields in reduced frequency for all values of slenderness ratio.

The effect of magnetic field length scale parameter on dimensionless frequency of MEVHT nanobeams is presented in Fig. 6. From this figure it can be witnessed that for different values of magnetic field intensity (H) considered, a higher value of length scale parameter yields a higher dimensionless frequency. Also, a larger value of H results in improved frequency.

5. Conclusions

This article studies the frequency response of MEVHT nanobeam through nonlocal strain gradient elasticity theory in association with the higher order refined beam theory. The governing equations are obtained via Hamilton's principle and solved analytically. The numerical assessment reveals that

(1) The natural frequency of MEVHT nanobeam exhibits a higher value when the higher value of length scale parameter is used. However, considering the nonlocal parameter appears to have detrimental effect.
(2) The critical damping co-efficient reduces for higher values of nonlocal parameter μ.
(3) With the higher magnitude of hygrothermal loads, the critical damping coefficient reduces.
(4) The natural frequency of MEVHT nanobeams is minimal at the lower slenderness ratio. Also, at all the slenderness ratio, the higher value of damping results in lesser frequency.
(5) A higher value of magnetic intensity improves the frequency response of MEVHT nanobeam

References

Akbarzadeh, A.H. and Chen, Z.T. (2013), "Hygrothermal stresses in one-dimensional functionally graded piezoelectric media in constant magnetic field", *Compos. Struct.*, **97**, 317-331. https://doi.org/10.1016/j.compstruct.2012.09.058

Alzahrani, E.O., Zenkour, A.M. and Sobhy, M. (2013), "Small scale effect on hygro-thermo-mechanical bending of nanoplates embedded in an elastic medium", *Compos. Struct.*, **105**, 163-172. https://doi.org/10.1016/j.compstruct.2013.04.045

Barati, M.R., Zenkour, A.M. and Shahverdi, H. (2016), "Thermo-mechanical buckling analysis of embedded nanosize FG plates in thermal environments via an inverse cotangential theory", *Compos. Struct.*, **141**, 203-212. https://doi.org/10.1016/j.compstruct.2016.01.056

Daie, M., Jalali, A., Suhatril, M., Shariati, M., Arabnejad Khanouki, M. M., Shariati, A. and Kazemi-Arbat, P. (2011), "A new finite element investigation on pre-bent steel strips as damper for vibration control", *Int. J. Phys. Sci.*, **6**(36), 8044-8050. https://doi.org/10.5897/IJPS11.1585

Ebrahimi, F. and Barati, M.R. (2016a), "Wave propagation analysis of quasi-3D FG nanobeams in thermal environment based on nonlocal strain gradient theory", *Appl. Phys. A*, **122**(9), 843. https://doi.org/10.1007/s00339-016-0368-1

Ebrahimi, F. and Barati, M.R. (2016b), "Size-dependent dynamic modeling of inhomogeneous curved nanobeams embedded in elastic medium based on nonlocal strain gradient theory", *Proceedings of the Institution of Mechanical Engineers, Part C: J. Mech. Eng. Sci.*, 0954406216668912. https://doi.org/10.1177/0954406216668912

Ebrahimi, F. and Barati, M.R. (2017a), "Hygrothermal effects on vibration characteristics of viscoelastic FG nanobeams based on nonlocal strain gradient theory", *Compos. Struct.*, **159**, 433-444. https://doi.org/10.1016/j.compstruct.2016.09.092

Ebrahimi, F. and Barati, M.R. (2017b), "A nonlocal strain gradient refined beam model for buckling analysis of size-dependent shear-deformable curved FG nanobeams", *Compos. Struct.*, **159**, 174-182. https://doi.org/10.1016/j.compstruct.2016.09.058

Ebrahimi, F. and Salari, E. (2015a), "Effect of various thermal loadings on buckling and vibrational characteristics of nonlocal temperature-dependent FG nanobeams", *Mech. Adv. Mater. Struct.*, **23**(12), 1379-1397. https://doi.org/10.1080/15376494.2015.1091524

Ebrahimi, F. and Salari, E. (2015b), "Thermo-mechanical vibration analysis of nonlocal temperature-dependent FG nanobeams with various boundary conditions", *Compos. Part B: Eng.*, **78**, 272-290. https://doi.org/10.1016/j.compositesb.2015.03.068

Ebrahimi, F., Barati, M.R. and Dabbagh, A. (2016), "A nonlocal strain gradient theory for wave propagation analysis in temperature-dependent inhomogeneous nanoplates", *Int. J. Eng. Sci.*, **107**, 169-182. https://doi.org/10.1016/j.ijengsci.2016.07.008

Eringen, A.C. (1983), "On differential equations of nonlocal elasticity and solutions of screw dislocation and surface waves", *J. Appl. Phys.*, **54**(9), 4703-4710. https://doi.org/10.1063/1.332803

Frikha, A., Zghal, S. and Dammak, F. (2018), "Dynamic analysis of functionally graded carbon nanotubes-reinforced plate and shell structures using a double directors finite shell element", *Aerosp. Sci. Technol.*, **78**, 438-451. https://doi.org/10.1016/j.ast.2018.04.048

Hamed, M.A., Eltaher, M.A., Sadoun, A.M. and Almitani, K.H. (2016), "Free vibration of symmetric and sigmoid functionally graded nanobeams", *Appl. Phys. A*, **122**(9), 829. https://doi.org/10.1007/s00339-016-0324-0

Hashemi, S.H., Mehrabani, H. and Ahmadi-Savadkoohi, A. (2015), "Exact solution for free vibration of coupled double viscoelastic graphene sheets by viscoPasternak medium", *Compos. Part B: Eng.*, **78**, 377-383. https://doi.org/10.1016/j.compositesb.2015.04.008

Heidari, R.M., Alimirzaei, S. and Torabi, K. (2015), "Analytical

solution for free vibration of functionally graded carbon nanotubes (FG-CNT) reinforced double-layered nano-plates resting on elastic medium".

Henderson, J.P., Plummer, A. and Johnston, N. (2018), "An electro-hydrostatic actuator for hybrid active-passive vibration isolation", *Int. J. Hydromechatron.*, **1**(1), 47-71.

Hosseini, M. and Jamalpoor, A. (2015), "Analytical solution for thermomechanical vibration of double-viscoelastic nanoplate-systems made of functionally graded materials", *J. Thermal Stress.*, **38**(12), 1428-1456. https://doi.org/10.1080/01495739.2015.1073986

Jalali, A., Daie, M., Nazhadan, S.V.M., Kazemi-Arbat, P. and Shariati, M. (2012), "Seismic performance of structures with pre-bent strips as a damper", *Int. J. Phys. Sci.*, **7**(26), 4061-4072. http://dx.doi.org/10.5897/IJPS11.1324

Khorami, M., Alvansazyazdi, M., Shariati, M., Zandi, Y., Jalali, A. and Tahir, M. (2017), "Seismic performance evaluation of buckling restrained braced frames (BRBF) using incremental nonlinear dynamic analysis method (IDA)." http://dx.doi.org/10.12989/eas.2017.13.6.531

Khorramian, K., Maleki, S., Shariati, M. and Ramli Sulong, N. H. (2015), "Behavior of Tilted Angle Shear Connectors", *PLoS One*, **10**(12), e0144288. http://dx.doi.org/10.1371/journal.pone.0144288

Lee, C.Y. and Kim, J.H. (2013), "Hygrothermal postbuckling behavior of functionally graded plates", *Compos. Struct.*, **95**, 278-282. https://doi.org/10.1016/j.compstruct.2012.07.010

Li, L., Hu, Y. and Ling, L. (2015), "Flexural wave propagation in small-scaled functionally graded beams via a nonlocal strain gradient theory", *Compos. Struct.*, **133**, 1079-1092. https://doi.org/10.1016/j.compstruct.2015.08.014

Li, D., Toghroli, A., Shariati, M., Sajedi, F., Bui, D.T., Kianmehr, P., Mohamad, E.T. and Khorami, M. (2019), "Application of polymer, silica-fume and crushed rubber in the production of Pervious concrete", *Smart Struct. Syst., Int. J.*, **23**(2), 207-214. http://dx.doi.org/10.12989/sss.2019.23.2.207

Lei, Y., Adhikari, S. and Friswell, M.I. (2013), "Vibration of nonlocal Kelvin–Voigt viscoelastic damped Timoshenko beams", *Int. J. Eng. Sci.*, **66**, 1-13. https://doi.org/10.1016/j.ijengsci.2013.02.004

Lim, C.W. (2010), "On the truth of nanoscale for nanobeams based on nonlocal elastic stress field theory: equilibrium, governing equation and static deflection", *Appl. Mathe. Mech.*, **31**(1), 37-54. https://doi.org/10.1007/s10483-010-0105-7

Luo, Z., Sinaei, H., Ibrahim, Z., Shariati, M., Jumaat, Z., Wakil, K., Pham, B.T., Mohamad, E.T. and Khorami, M. (2019), "Computational and experimental analysis of beam to column joints reinforced with CFRP plates", *Steel Compos. Struct., Int. J.*, **30**(3), 271-280. http://dx.doi.org/10.12989/scs.2019.30.3.271

Mansouri, M.H. and Shariyat, M. (2015), "Biaxial thermo-mechanical buckling of orthotropic auxetic FGM plates with temperature and moisture dependent material properties on elastic foundations", *Compos. Part B: Eng.*, **83**, 88-104. https://doi.org/10.1016/j.compositesb.2015.08.030

Mansouri, I., Shariati, M., Safa, M., Ibrahim, Z., Tahir, M. and Petković, D. (2019), "Analysis of influential factors for predicting the shear strength of a V-shaped angle shear connector in composite beams using an adaptive neuro-fuzzy technique", *J. Intel. Manuf.*, **30**(3), 1247-1257. https://doi.org/10.1007/s10845-017-1306-6

Mahmoud, S.R., Chaht, F.L., Kaci, A., Houari, M.S.A., Tounsi, A. and Bég, O.A. (2015), "Bending and buckling analyses of functionally graded material (FGM) size-dependent nanoscale beams including the thickness stretching effect", *Steel Compos. Struct., Int. J.*, **18**(2), 425-442. https://doi.org/10.12989/scs.2015.18.2.425

Mantari, J.L., Bonilla, E.M. and Soares, C.G. (2014), "A new tangential-exponential higher order shear deformation theory for advanced composite plates", *Compos. Part B: Eng.*, **60**, 319-328. https://doi.org/10.1016/j.compositesb.2013.12.001

Milovančević, M., Marinović, J.S., Nikolić, J., Kitić, A., Shariati, M., Trung, N.T., Wakil, K. and Khorami, M. (2019), "UML diagrams for dynamical monitoring of rail vehicles", *Physica A: Statist. Mech. Applicat.*, **53**, 121169. https://doi.org/10.1016/j.physa.2019.121169

Rahmani, O. and Pedram, O. (2014), "Analysis and modeling the size effect on vibration of functionally graded nanobeams based on nonlocal Timoshenko beam theory", *Int. J. Eng. Sci.*, **77**, 55-70. https://doi.org/10.1016/j.ijengsci.2013.12.003

Safa, M., Shariati, M., Ibrahim, Z., Toghroli, A., Baharom, S.B., Nor, N.M. and Petkovic, D. (2016), "Potential of adaptive neuro fuzzy inference system for evaluating the factors affecting steel-concrete composite beam's shear strength", *Steel Compos. Struct., Int. J.*, **21**(3), 679-688. https://doi.org/10.12989/scs.2016.21.3.679

Safa, M., Sari, P.A., Shariat, M., Suhatril, M., Trung, N.T., Wakil, K. and Khorami, M. (2020), "Development of neuro-fuzzy and neuro-bee predictive models for prediction of the safety factor of eco-protection slopes", *Physica A.* https://doi.org/10.1016/j.physa.2019.124046

Sedghi, Y., Zandi, Y., Shariati, M., Ahmadi, E., Moghimi Azar, V., Toghroli, A., Safa, M., Tonnizam Mohamad, E., Khorami, M. and Wakil, K. (2018), "Application of ANFIS technique on performance of C and L shaped angle shear connectors", *Smart Struct. Syst., Int. J.*, **22**(3), 335-340. http://dx.doi.org/10.12989/sss.2018.22.3.335

Shah, S., Sulong, N.R., Jumaat, M. and Shariati, M. (2016a), "State-of-the-art review on the design and performance of steel pallet rack connections", *Eng. Fail. Anal.*, **66**, 240-258. https://doi.org/10.1016/j.engfailanal.2016.04.017

Shah, S., Sulong, N.R., Shariati, M., Khan, R. and Jumaat, M. (2016b), "Behavior of steel pallet rack beam-to-column connections at elevated temperatures", *Thin-Wall. Struct.*, **106**, 471-483. https://doi.org/10.1016/j.tws.2016.05.021

Shahabi, S., Sulong, N., Shariati, M., Mohammadhassani, M. and Shah, S. (2016), "Numerical analysis of channel connectors under fire and a comparison of performance with different types of shear connectors subjected to fire", *Steel Compos. Struct., Int. J.*, **20**(3), 651-669. https://doi.org/10.12989/scs.2016.20.3.651

Shao, Z., Wakil, K., Usak, M., Amin Heidari, M., Wang, B. and Simoes, R. (2018), "Kriging Empirical Mode Decomposition via support vector machine learning technique for autonomous operation diagnosing of CHP in microgrid", *Appl. Thermal Eng.*, **145**, 58-70. https://doi.org/10.1016/j.applthermaleng.2018.09.028

Shariati, A., Ramli Sulong, N.H., Suhatril, M. and Shariati, M. (2012a), "Investigation of channel shear connectors for composite concrete and steel T-beam", *Int. J. Phys. Sci.*, **7**(11), 1828-1831. https://doi.org/10.5897/IJPS11.1604

Shariati, M., Ramli Sulong, N., Suhatril, M., Shariati, A., Arabnejad Khanouki, M. and Sinaei, H. (2012b), "Fatigue energy dissipation and failure analysis of channel shear connector embedded in the lightweight aggregate concrete in composite bridge girders", *Procedings of the 5th International Conference on Engineering Failure Analysis*, Hilton Hotel, The Hague, The Netherlands, July.

Shariati, M., Shariati, A., Sulong, N.R., Suhatril, M. and Khanouki, M.A. (2014), "Fatigue energy dissipation and failure analysis of angle shear connectors embedded in high strength concrete", *Eng. Fail. Anal.*, **41**, 124-134. https://doi.org/10.1016/j.engfailanal.2014.02.017

Shariati, M., Trung, N.T., Wakil, K., Mehrabi, P., Safa, M. and Khorami, M. (2019a), "Estimation of moment and rotation of

steel rack connections using extreme learning machine", *Steel Compos. Struct., Int. J.*, **31**(5), 427-435. https://doi.org/10.12989/scs.2019.31.5.427

Shariati, M., Safaei Faegh, S., Mehrabi, P., Bahavarnia, S., Zandi, Y., Rezaee Masoom, D., Toghroli, A., Trung, N.T. and Salih, M.N. (2019b), "Numerical study on the structural performance of corrugated low yield point steel plate shear walls with circular openings", *Steel Compos. Struct., Int. J.*, **33**(4), 569-581. https://doi.org/10.12989/scs.2019.33.4.569

Shariati, M., Mafipour, M.S., Mehrabi, P., Shariati, A., Toghroli, A., Trung, N.T. and Salih, M.N.A. (2020), "A novel approach to predict shear strength of tilted angle connectors using artificial intelligence techniques", *Eng. Comput.*, 1-21. https://doi.org/10.1007/s00366-019-00930-x

Shi, X., Hassanzadeh-Aghdam, M.K. and Ansari, R. (2019a), "Viscoelastic analysis of silica nanoparticle-polymer nanocomposites", *Compos. Part B: Eng.*, **158**, 169-178. https://doi.org/10.1016/j.compositesb.2018.09.084

Shi, X., Jaryani, P., Amiri, A., Rahimi, A. and Malekshah, E.H. (2019b), "Heat transfer and nanofluid flow of free convection in a quarter cylinder channel considering nanoparticle shape effect", *Powder Technol.*, **346**, 160-170. https://doi.org/10.1016/j.powtec.2018.12.071

Şimşek, M. and Yurtcu, H.H. (2013), "Analytical solutions for bending and buckling of functionally graded nanobeams based on the nonlocal Timoshenko beam theory", *Compos. Struct.*, **97**, 378-386. https://doi.org/10.1016/j.compstruct.2012.10.038

Sobhy, M. (2015a), "Hygrothermal vibration of orthotropic double-layered graphene sheets embedded in an elastic medium using the two-variable plate theory", *Appl. Mathe. Model.*, **40**(1), 85-99. https://doi.org/10.1016/j.apm.2015.04.037

Sobhy, M. (2015b), "Thermoelastic Response of FGM Plates with Temperature-Dependent Properties Resting on Variable Elastic Foundations", *Int. J. Appl. Mech.*, **7**(6), 1550082. https://doi.org/10.1142/S1758825115500829

Suhatril, M., Osman, N., Sari, P.A., Shariati, M. and Marto, A. (2019), "Significance of surface eco-protection techniques for cohesive soils slope in Selangor, Malaysia", *Geotech. Geol. Eng.*, **37**(3), 2007-2014. https://doi.org/10.1007/s10706-018-0740-3

Tanaka, Y. (2018), "Active vibration compensator on moving vessel by hydraulic parallel mechanism", *Int. J. Hydromechatro.*, **1**(3), 350-359. https://doi.org/10.1504/IJHM.2018.094887

Trabelsi, S, Frikha, A., Zghal, S. and Dammak, F. (2019), "A modified FSDT-based four nodes finite shell element for thermal buckling analysis of functionally graded plates and cylindrical shells", *Eng. Struct.*, **178**, 444-459. https://doi.org/10.1016/j.engstruct.2018.10.047

Trung, N.T., Shahgoli, A.F., Zandi, Y., Shariati, M., Wakil, K., Safa, M. and Khorami, M. (2019), "Moment-rotation prediction of precast beam-to-column connections using extreme learning machine", *Struct. Eng. Mech., Int. J.*, **70**(5), 639-647. https://doi.org/10.12989/sem.2019.70.5.639

Vinyas, M. and Kattimani, S.C. (2018a), "Investigation of the effect of $BaTiO_3/CoFe_2O_4$ particle arrangement on the static response of magneto-electro-thermo-elastic plates", *Compos. Struct.*, **185**(1), 51-64. https://doi.org/10.1016/j.compstruct.2017.10.073

Vinyas, M. and Kattimani, S.C. (2018b), "Hygrothermal analysis of magneto-electro-elastic plate using 3D finite element analysis", *Compos. Struct.*, **180**, 617-637. https://doi.org/10.1016/j.compstruct.2017.08.015

Vinyas, M. and Kattimani, S.C. (2018c), "Finite element evaluation of free vibration characteristics of magneto-electro-elastic rectangular plates in hygrothermal environment using higher-order shear deformation theory", *Compos. Struct.*, **202**, 1339-1352. https://doi.org/10.1016/j.compstruct.2018.06.069

Vinyas, M., Kattimani, S.C., Loja, M.A.R. and Vishwas, M. (2018), "Effect of $BaTiO_3/CoFe_2O_4$ micro-topological textures on the coupled static behaviour of magneto-electro-thermo-elastic beams in different thermal environment", *Mater. Res. Express*, **5**, 125702. https://doi.org/10.1088/2053-1591/aae0c8

Xu, C., Zhang, X., Haido, J.H., Mehrabi, P., Shariati, A., Mohamad, E.T., Hoang, N. and Wakil, K. (2019), "Using genetic algorithms method for the paramount design of reinforced concrete structures", *Struct. Eng. Mech., Int. J.*, **71**(5), 503-513. https://doi.org/10.12989/sem.2019.71.5.503

Yan, Z. and Jiang, L.Y. (2012), "Vibration and buckling analysis of a piezoelectric nanoplate considering surface effects and in-plane constraints", *Proceedings of the Royal Society A: Mathematical, Phys. Eng. Sci.*, **468**(2147), 3458-3475. https://doi.org/10.1098/rspa.2012.0214

Zandi, Y., Shariati, M., Marto, A., Wei, X., Karaca, Z., Dao, D., Toghroli, A., Hashemi, M.H., Sedghi, Y. and Wakil, K. (2018), "Computational investigation of the comparative analysis of cylindrical barns subjected to earthquake", *Steel Compos. Struct., Int. J.*, **28**(4), 439-447. http://dx.doi.org/10.12989/scs.2018.28.4.439

Zemri, A., Houari, M.S.A., Bousahla, A.A. and Tounsi, A. (2015), "A mechanical response of functionally graded nanoscale beam: an assessment of a refined nonlocal shear deformation theory beam theory", *Struct. Eng. Mech., Int. J.*, **54**(4), 693-710. https://doi.org/10.12989/sem.2015.54.4.693

Zenkour, A. (2013), "Hygrothermal analysis of exponentially graded rectangular plates", *J. Mech. Mater. Struct.*, **7**(7), 687-700. 1 https://doi.org/100.2140/jomms.2012.7.687

Zenkour, A.M., Allam, M.N.M. and Radwan, A.F. (2014), "Effects of transverse shear and normal strains on fg plates resting on elastic foundations under hygro-thermo-mechanical loading", *Int. J. Appl. Mech.*, **6**(5), 1450063. https://doi.org/10.1142/S175882511450063X

Zghal, S., Frikha, A. and Dammak, F. (2018), "Mechanical buckling analysis of functionally graded power-based and carbon nanotubes-reinforced composite plates and curved panels", *Compos. Part B: Eng.*, **150**, 165-183. https://doi.org/10.1016/j.compositesb.2018.05.037

Zhang, J. and Wang, C. (2012), "Vibrating piezoelectric nanofilms as sandwich nanoplates", *J. Appl. Phys.*, **111**(9), 094303. https://doi.org/10.1063/1.4709754

CC